

Cytotoxicity of the matrix metalloproteinase-activated anthrax lethal toxin is dependent on gelatinase expression and B-RAF status in human melanoma cells

Randall W. Alfano,^{1,2} Stephen H. Leppla,³ Shihui Liu,³ Thomas H. Bugge,⁴ Meenhard Herlyn,⁵ Keiran S. Smalley,⁵ Jennifer L. Bromberg-White,⁶ Nicholas S. Duesbery,⁶ and Arthur E. Frankel^{1,2}

¹Scott & White Cancer Research Institute Memorial Hospital; ²Department of Internal Medicine, Texas A&M Health Science Center, Temple, Texas; ³Laboratory of Bacterial Diseases, National Institute of Allergy and Infectious Diseases; ⁴Oral and Pharyngeal Cancer Branch, National Institute of Dental and Craniofacial Research, NIH, Bethesda, Maryland; ⁵The Wistar Institute, Philadelphia, Pennsylvania; and ⁶Laboratory of Cancer and Developmental Cell Biology, Van Andel Research Institute, Grand Rapids, Michigan

Abstract

Anthrax lethal toxin (LeTx) shows potent mitogen-activated protein kinase pathway inhibition and apoptosis in melanoma cells that harbor the activating V600E B-RAF mutation. LeTx is composed of two proteins, protective antigen and lethal factor. Uptake of the toxin into cells is dependent on proteolytic activation of protective antigen by the ubiquitously expressed furin or furin-like proteases. To circumvent nonspecific LeTx activation, a substrate preferably cleaved by gelatinases was substituted for the furin LeTx activation site. Here, we have shown that the toxicity of this matrix metalloproteinase (MMP)-activated LeTx is dependent on host cell surface MMP-2 and MMP-9 activity as well as the presence of the activating V600E B-RAF mutation, making this toxin dual specific. This additional layer of tumor cell specificity would potentially decrease systemic toxicity from the reduction of nonspecific toxin activation while retaining antitumor efficacy in patients with V600E B-RAF melanomas. Moreover, our results indicate that cell surface-associated gelatinase expression can be used to predict sensitivity among V600E

B-RAF melanomas. This finding will aid in the better selection of patients that will potentially respond to MMP-activated LeTx therapy. [Mol Cancer Ther 2008;7(5):1218–26]

Introduction

Chemotherapeutic regimens have limited activity in metastatic melanoma patients. Response rates are currently between 10% and 25% with median survival of 8 months for single agent dacarbazine and no apparent benefit can be seen with polychemotherapy or biochemotherapy (1). Furthermore, interleukin-2 and IFN- α addition to chemotherapy improves response rate and progression-free survival only in a select few patients (1). The poor clinical performance of these traditional treatments has led to the development of agents that specifically target protein components of molecular pathways that drive melanoma proliferation and dissemination. Mutations leading to the constitutive activation of the mitogen-activated protein kinase (MAPK) pathway are common in melanoma. A specific valine-to-glutamic acid substitution at amino acid position 600 of the B-RAF protein component constitutively activates this pathway, resulting in loss of cell proliferation control (2). Enzymes implicated in melanoma metastasis are matrix metalloproteinases (MMP). The extracellular matrix degrading function of these enzymes positively correlates with poor prognosis in melanoma patients (3). Further, activation of MAPK in melanomas causes increased MMP expression (4). Small molecular weight inhibitors, which separately target these two pathways, have been tested in melanomas but have yielded little clinical benefit (2, 4). We therefore sought a more potent agent that targets these tumor systems.

We examined recombinant toxin compounds for melanoma therapy based on their extreme catalytic potency and the prior experience of our laboratories. Anthrax lethal toxin (LeTx), secreted from the Gram-positive *Bacillus anthracis*, shows potent MAPK pathway inhibition (5). LeTx is composed of two proteins, the 83-kDa protective antigen (PA) and the 90-kDa lethal factor (LF). Toxin uptake into cells is dependent on proteolytic activation of PA by ubiquitously expressed furin or furin-like proteases after PA binding to one of two widely expressed receptors, capillary morphogenesis gene 2 and tumor endothelial marker 8 (6). The activated PA subsequently heptamerizes, binds three LF molecules, and migrates into lipid rafts where subsequent internalization occurs. Progressive acidification of the early endosome induces PA heptamer pore formation and subsequent LF escape into the cytosol (7).

Received 1/9/08; revised 2/22/08; accepted 2/29/08.

Grant support: Scott & White Cancer Research Institute.

The costs of publication of this article were defrayed in part by the payment of page charges. This article must therefore be hereby marked *advertisement* in accordance with 18 U.S.C. Section 1734 solely to indicate this fact.

Requests for reprints: Arthur E. Frankel, Scott & White Cancer Research Institute, 5701 South Airport Road, Temple, TX 76502. Phone: 254-724-0094; Fax: 254-724-2324. E-mail: afrankel@swmail.sw.org

Copyright © 2008 American Association for Cancer Research.

doi:10.1158/1535-7163.MCT-08-0024

The catalytic activity of LF causes the cleavage and inactivation of the MEKs, with the exception of MEK5, and thus the complete inhibition of all three branches of the MAPK pathway (8). LeTx induces cell cycle arrest and triggers apoptosis in human melanoma cells (9, 10). However, specificity in both tissue culture and animal models was limited due to the presence of receptors on many normal tissues and the ubiquitous expression of furin. Hence, we needed to provide an additional layer of specificity to LeTx to improve the melanoma therapeutic index *in vivo*. Efforts have recently been taken to enhance the specificity of LeTx (11, 12). Liu et al. modified LeTx by changing the furin cleavage sequence of PA, ¹⁶⁴RKKR¹⁶⁷, to a gelatinase (MMP-2/9) selective cleavage sequence, ¹⁶⁴GPLGMLSQ¹⁷¹. The engineered PA, PA-L1, when combined with LF retained melanoma cell cytotoxicity (11). In addition, it was 3-fold less toxic to mice and had a 20-fold longer circulating half-life (11). At maximal tolerated doses, human C32 melanoma xenografts showed 90% tumor growth inhibition and 30% complete regressions with PA-L1/LF but no tumor growth inhibition with LeTx. The theoretical dual specificity of PA-L1/LF should provide a safe and effective melanoma therapeutic for a specific subset of patients. To confirm the molecular mechanism of the drug and identify biomarkers for patient identification, we undertook this study to examine the potency of PA-L1/LF in a series of human melanoma cell lines. Cell sensitivities to PA-L1/LF were correlated with the MMP-2/9 activity levels as well as the presence of the B-RAF V600E mutation.

Materials and Methods

Reagents

PA, PA-L1, LF, FP59, and LF- β -Lac were produced as described previously (13–15). FP59 consists of the first 254 amino acids of LF (the PA/PA-L1 binding domain) fused to the catalytic portion of *Pseudomonas* exotoxin A (amino acids 362–613; ref. 15). FP59 when internalized in a PA/PA-L1-dependent mechanism inhibits protein synthesis and thus is toxic to all cells (15). The fusion protein LF- β -Lac consists of the PA binding domain of LF genetically fused to the β -lactamase enzyme (13).

Cell Lines and Cell Culture

The melanoma cell lines WM793B, WM46, WM983A, WM51, WM902B, WM1158, WM239A, WM3211, WM852, and WM1361A are from the Wistar Institute collection and were maintained in 2% tumor medium (4:1 MCDB153 with 1.5 g/L sodium bicarbonate and Leibovitz's L-15 medium with 2 mmol/L L-glutamine, 0.005 mg/mL bovine insulin, 1.68 mmol/L CaCl₂, 2% fetal bovine serum). Cell lines C32, SK-MEL-24, WM115, Malme-3M, HT-144, WM-266-4, A2058, A375, 1205Lu, 451Lu, G361, A101D, SK-MEL-28, and SK-MEL-2 were purchased from the American Type Culture Collection and grown as recommended. The cell line SK-MEL-173 was provided by Dr. Alan Houghton (Sloan Kettering) and cultured in RPMI 1640 plus 10% FBS. All cells were maintained at 37°C in a 5% CO₂ environment.

Cytotoxicity Assay

The [³H]thymidine incorporation inhibition assay was used as described previously (10). Briefly, cell lines were progressively weaned from serum-containing medium to AIMV serum-free medium (Invitrogen) as recommended by the manufacturer. Ten thousand cells per well were plated in 25% recommended medium/75% AIMV in Costar 96-well flat-bottomed plates. Cells were allowed to adhere to the plate, and the medium was exchanged for 100% AIMV containing 1 nmol/L LF/FP59. Serially diluted PA/PA-L1 ranging from a final concentration of 0 to 10,000 pmol/L was added. After 48 h at 37°C, 5% CO₂, 1 μ Ci [³H]thymidine (NEN DuPont) in 50 μ L/well AIMV was added and incubated at 37°C, 5% CO₂ for an additional 18 h. The cells were then harvested with a Skatron Cell Harvester (Skatron Instruments) onto glass fiber mats, and counts/min of incorporated [³H]thymidine were quantified using a LKB liquid scintillation counter gated for ³H (Perkin-Elmer). Concentration of toxin that inhibited [³H]thymidine incorporation by 50% compared with control wells defined the IC₅₀. The percent maximal [³H]thymidine incorporation was plotted versus the log of the toxin concentrations, and nonlinear regression with a variable slope sigmoidal dose-response curve was generated along with IC₅₀ using GraphPad Prism software (GraphPad Software). Assays were done in triplicate with IC₅₀ variability between assays of <30%.

PA-L1/LF- β -Lac Fluorescence Resonance Energy Transfer Flow Cytometry

Cells (250,000 per well) were plated in a Costar 12-well plates in 25% recommended medium/75% AIMV. Cells were allowed to adhere to the plate at 37°C, 5% CO₂ and washed once with AIMV, and fresh AIMV medium was added. Cells were then incubated overnight at 37°C, 5% CO₂. LF- β -Lac alone (90 nmol/L) or PA-L1 (26 nmol/L)/LF- β -Lac (90 nmol/L) was added to the conditioned medium and incubated for 5 h at 37°C, 5% CO₂. Cells were then washed twice with AIMV and loaded with CCF-2/AM (Invitrogen) for 1 h at room temperature in the dark using the alternative loading protocol as described by the manufacturer. After four washes with AIMV/2 mmol/L Probenicid (Sigma), the culture medium was replaced with AIMV/2 mmol/L Probenicid, which was incubated at room temperature in the dark for an additional 75 min to allow for fluorescence resonance energy transfer (FRET) disruption. Cells were then trypsinized using 0.25% trypsin/EDTA (Invitrogen), washed twice with ice-cold HBSS (Invitrogen) containing 2 mmol/L Probenicid, and resuspended in HBSS/2 mmol/L Probenicid at a concentration of 500,000 cells/mL. Analysis was done using BD FACSaria flow cytometer (BD Biosciences) and data were analyzed by Diva (BD Biosciences). Cell lines were compared by using the mean blue fluorescence intensity of the PA-L1/LF- β -Lac-treated cells, which was adjusted for nonspecific CCF-2/AM cleavage using the mean blue fluorescence of the LF- β -Lac-treated negative controls and subsequently divided by the mean green fluorescence of the LF- β -Lac-negative controls adjusted for autofluorescence of

unstained, untreated controls times 100 to generate percent control mean blue fluorescence.

PA-L1/LF- β -Lac FRET Microscopy

The PA-L1/LF- β -Lac FRET disruption assay was visualized via fluorescent microscopy. Two hundred thousand cells were plated in eight-well chamber slides (Lab-tek) in 25% recommended medium/75% AIMV. The cells were allowed to adhere and washed once with AIMV, and culture medium was replaced with AIMV. Cells were incubated overnight at 37°C, 5% CO₂ and 26 nmol/L PAL1/90 nmol/L LF- β -Lac was subsequently added to the conditioned medium. Cells were incubated at 37°C, 5% CO₂ for 5 h. Cells were washed twice with AIMV and loaded with CCF-2/AM using the alternative loading protocol as recommended by the manufacturer for 1 h at room temperature. Cells were then washed four times with AIMV/2 mmol/L Probenicid and incubated at room temperature for an additional 75 min to allow for FRET disruption in fresh AIMV/2 mmol/L Probenicid. The culture medium was removed and the cells were visualized with a BX51 fluorescent microscope (Olympus) fitted with excitation filter HQ405/20 nm band-pass, dichroic 425DCXR, emission filter HQ460/40 nm (Chroma Technology) for blue fluorescence acquisition. For green image acquisition, excitation filter HQ405/20 nm band-pass, dichroic 425DCXR, emission filter HQ530/30 nm (Chroma Technology) using a $\times 10$ objective for a total magnification of $\times 100$. Images were obtained with a DP71 digital camera (Olympus) using the same exposure time for each cell line and subsequently analyzed using DP manager (Olympus).

Gelatin Zymography

Gelatin zymography was done as described previously (14). Briefly, for cell lysate analysis of MMP-2/9 levels, 80% to 100% confluent T-150 flasks of cells were progressively weaned to 100% AIMV. Cells were lysed on ice for 10 min using 1.5 mL lysis buffer per flask [0.5% (v/v) Triton X-100 in 0.1 mol/L Tris-HCl (pH 8.1)] and removed with a rubber scraper. Cell lysates were spun at 10,000 rpm using an Allegra 2502 centrifuge fitted with TA-10-250 rotor (Beckman Coulter). Cell lysate protein concentration was equilibrated to 0.65 mg/mL using the BCA procedure (Pierce). The lysate fraction contained plasma membrane sheets and vesicles; therefore, MMP-2/9 activities in the cell lysate were considered as cell surface gelatinase activities. For conditioned medium zymography, 4 million cells were incubated in 5 mL AIMV for 20 h at 37°C, 5% CO₂. The culture medium was harvested and spun at 10,000 rpm at 4°C using an Allegra 2502 centrifuge fitted with TA-10-250 rotor (Beckman Coulter). For concentration of gelatinases, conditioned medium/1 mg cell lysate protein was incubated with 50 μ L gelatin Sepharose beads (GE) in equilibration buffer [50 mmol/L Tris-HCl, 150 mmol/L NaCl, 5 mmol/L CaCl₂, 0.02% (v/v) Tween 20, 10 mmol/L EDTA (pH 7.6)] for 1 h at 4°C on an end-over-end mixer.

Cell lysates/conditioned medium were spun at 500 RCF for 10 min at 4°C using a Microfuge 18 centrifuge (Beckman Coulter) and resuspended in 500 μ L wash buffer [50 mmol/L Tris-HCl, 200 mmol/L NaCl, 5 mmol/L CaCl₂, 0.02% (v/v)

Tween 20, 10 mmol/L EDTA (pH 7.6)]. After four washes with wash buffer, beads were resuspended in 30 μ L of 2 \times Tris-glycine sample buffer (Invitrogen) and loaded in 10% gelatin zymogram gel (Invitrogen). Gels were run at 125 mV for 90 min and developed according to Invitrogen. Positive controls consisted of recombinant 68-kDa proform (Millipore) and 62-kDa active form (Calbiochem) of MMP-2 and the 92-kDa proform (Millipore) and 83-kDa active form (Calbiochem) MMP-9. MMP-2/9 band density was determined with the Fluorchem SP densitometer (Alpha Innotech) and calculated as a percent of the intensity of the recombinant gelatinase. Total gelatinase activity was calculated as the average of the percent control standard MMP-2 and MMP-9 of each cell line.

Western Blot

Cells were seeded in T-75 flasks and weaned to 100% AIMV. Cells were lysed in RIPA lysis buffer [0.5 mol/L Tris (pH 7.4), 0.25% Triton X-100, 0.02 mol/L sodium deoxycholate, 0.15 mol/L NaCl, 1 mmol/L EDTA] plus complete protease inhibitors (Roche). Cell lysates were equilibrated using the BCA procedure (Pierce) to 2 mg/mL. Westerns were done as described previously using primary antibodies for PTEN (Cell Signaling Technology), MMP-1, and MT1-MMP (Abcam; ref. 10). Band intensity was determined by the Fluorchem SP densitometer (Alpha Innotech). Verification of equal loading was done using an anti- β -actin monoclonal antibody (Sigma).

Melanoma MAPK Mutational Status

Melanoma cells were grown to $\sim 80\%$ confluence, trypsinized, and incubated at 55°C for 3 h in DNA extraction buffer [400 mmol/L NaCl, 10 mmol/L Tris-HCl (pH 7.4), 10 mmol/L EDTA] containing 50 μ g/mL RNase A, 2% SDS, and 50 μ g/mL proteinase K. Cells were then sheared using an 18 G needle, extracted twice in phenol/chloroform/isoamyl alcohol (25:25:1), and chloroform was extracted. DNA concentrations were determined by spectrophotometry at 260 nm after ethanol precipitation.

For B-RAF mutation analysis of both exons 11 and 15, PCR on total DNA was carried out in the presence of 1 μ mol/L of both B-RAF forward primer Braf11F (5'-CTCTCAGGCATAAGGTAATGTAC-3') and B-RAF reverse primer Braf11R (5'-GAGTCCCGACTGCTGTGAAC-3') for exon 11. Exon 15 primers were forward primer Braf15F (5'-TCATAATGCTTGTCTGATAGGA-3') and reverse primer Braf15R (5'-GGCCAAAATTTAAT-CAGTGGA-3'). Reactions were done in 50 μ L volumes consisting of 5 μ L of 10 \times PCR buffer, 300 nmol/L of each nucleotide, 10 μ L of 5 \times Q solution, and 1.25 units Proofstart Taq (Qiagen). Exon 11 amplification was done by 95°C for 12 min followed by 35 cycles of 95°C for 45 s, 54°C for 90 s, and 72°C for 90 s and a final extension cycle of 72°C 3 min. Exon 15 amplification was done by 95°C for 12 min followed by 40 cycles of 95°C for 45 s, 56°C for 90 s, and 72°C for 90 s and a final extension cycle of 72°C for 3 min.

For NRAS mutation analysis, 1 μ mol/L of the NrasX3F (5'-CACACCCCCAGGATTCTTAC-3') and NrasX3R (5'-GTCCAAAGTCATTCCCAGTAG-3') were used to amplify

exon 3. Reaction mixtures were identical to B-RAF gene amplification and subjected to 94°C for 12 min followed by 8 cycles of 94°C for 45 s. Annealing temperature was decreased from 65°C by 2°C every 2 cycles to 59°C for 90 s followed by 72°C for 90 s, 25 cycles of 94°C for 45 s, 57°C for 90 s, 72°C for 90 s, and a final extension cycle of 72°C for 3 min. Correct PCR product size (403 bp for B-RAF exon 11, 233 bp for B-RAF exon 15, and 438 bp for NRAS exon 3) was verified by agarose gel electrophoresis. Sequences were verified using the ABI 3700 capillary electrophoresis DNA sequencer (Applied Biosystems).

Statistical Analysis

Significance of correlations was done using GraphPad Prism software (GraphPad Software). All analyses were done assuming Gaussian populations with a 95% confidence interval.

Results

PA-L1/LF Cytotoxicity to Melanoma Cells

We tested a panel of 25 melanoma cell lines for sensitivity to PA-L1/LF, PA/LF, and PA/FP59 (Table 1). FP59 consists of the PA binding domain of LF (amino acids 1-254) genetically fused to the ADP-ribosylation domain of *Pseudomonas* exotoxin A (amino acids 362-613) and is toxic to all cells in which it becomes internalized (15). Sensitivity to PA/FP59 indicated adequate LeTx receptor expression, whereas PA/LF sensitivity confirmed MAPK dependence of the target cell. Cytotoxicity analysis revealed that 12 of 25 cell lines were sensitive to PA-L1/LF. From our experience in clinical application of immunotoxins, we arbitrarily set sensitivity at an IC₅₀ <200 pmol/L with <10% of control [³H]thymidine incorporation at 10 nmol/L PA-L1/1 nmol/L LF (Table 1A; ref. 16). In determining the cause of PA-L1/LF resistance in the remaining 13 insensitive cell

Table 1. PA-L1/LF, PA/LF, and PA/FP59 induced proliferation inhibition and cytotoxicity of human melanoma cell lines

Cell line	PA-L1/LF ([³ H]thymidine, pmol/L)	PA/LF IC ₅₀ ([³ H]thymidine, pmol/L)	PA/FP59 IC ₅₀ ([³ H]thymidine, pmol/L)	MAPK pathway mutational status	Reference
(A) PA-L1/LF-sensitive melanoma cell lines					
SK-MEL-24	7	2	2	V600E B-RAF	(10)
WM793B	11	7	1	V600E B-RAF	(29)
C32	11	8	1	V600E B-RAF	(10)
WM115	19	8.7	0.65	V600E B-RAF	(25)
WM46	55	12	7.8	V600E B-RAF	
Malme-3M	64	54	25	V600E B-RAF	(10)
HT-144	104	25	2	V600E B-RAF	(10)
WM983A	109	16	5.1	V600E B-RAF	(10)
WM-266-4	119	58	5	V600E B-RAF	(10)
1205Lu	147	14	2	V600E B-RAF	(29)
WM852	159	14	0.7	Q61R NRAS	
WM51	177	54	15	V600E B-RAF	
(B) PA-L1/LF-resistant, PA/LF-sensitive melanoma cell lines					
G361	225	44	9	V600E B-RAF	(10)
A375	247	93	4	V600E B-RAF	(10)
A101D	335	30	3	V600E B-RAF	
SK-MEL-28	359	15	2	V600E B-RAF	(10)
451Lu	841	57	5.7	V600E B-RAF	(30)
WM902B	1,010	33	10	V600E B-RAF	
(C) PA/LF-resistant melanoma cell lines					
SK-MEL-2	407	319	130	Q61K NRAS	(10)
WM1361A	419	248	4.7	Q61R NRAS	(29)
SK-MEL-173	757	286	6.4	Wild-type B-RAF	
A2058	>10,000	>10,000	1.9	Heterozygous V600E B-RAF	
WM1158	>10,000	>10,000	0.5	V600E B-RAF	
WM239A	>10,000	>10,000	0.4	Wild-type B-RAF	
WM3211	>10,000	>10,000	1	Wild-type B-RAF/NRAS	

NOTE: PA-L1/LF, PA/LF, and PA/FP59 cytotoxicity to human melanoma cells. Twenty-five melanoma cell lines were tested for PA-L1/LF sensitivity as described in Materials and Methods. Assays were done in triplicate with IC₅₀ variability between assays of <30% and the IC₅₀ values were subsequently tabulated. (A) Twelve cell lines were sensitive to PA-L1/LF as well as PA/LF (IC₅₀ <200 pmol/L with <10% of control [³H]thymidine incorporation at 10 nmol/L PA-L1/1 nmol/L LF), whereas 13 melanomas were resistant to PA-L1/LF. (B) The PA-L1/LF-resistant cell lines G361, A375, A101D, SK-MEL-28, 451Lu, and WM902B were sensitive to PA/LF (IC₅₀ <200 pmol/L with <10% of control [³H]thymidine incorporation at 10 nmol/L PA/1 nmol/L LF) and thus exhibited MAPK dependency. (C) The PA-L1-resistant SK-MEL-2 showed resistance to PA/FP59, which suggested low LeTx receptor expression. The PA/FP59-sensitive WM1361A, SK-MEL-173, A2058, WM1158, WM239A, and WM3211 were not sensitive to PA/LF, which indicated tolerance for LF-mediated MAPK inhibition.

lines (Table 1B and C), both PA/FP59 and PA/LF cytotoxicity were compared. With the exception of SK-MEL-2 (PA/FP59 IC₅₀, 130 pmol/L), all cell lines exhibited adequate receptor expression for FP59 intoxication (Table 1C).

PA/LF cytotoxicity analysis revealed that 18 cell lines were sensitive to LF-mediated MEK cleavage, including the 12 PA-L1/LF-sensitive melanomas (IC₅₀ < 200 pmol/L with <10% of control [³H]thymidine incorporation at 10 nmol/L PA/1 nmol/L LF; Table 1A and B). These results are in agreement with previously published data from our laboratory and others in that the majority of the PA/LF-sensitive cells are positive for the signature B-RAF V600E mutation (10, 11). More importantly, 6 cell lines that were sensitive to PA/LF were resistant to PA-L1/LF (Table 1B). In addition, 6 cell lines were resistant to PA/LF as well as PA-L1/LF (Table 1C). Representative melanoma cell lines are shown from each group of cell lines in Supplementary Fig. S1.⁷

PA-L1/LF-Sensitive Melanomas Show High PA-L1 Activation

Because PA-L1 activation is required for its oligomerization and LF binding, decreased PA-L1 activation may lead to reduced LF internalization. Therefore, to determine whether PA-L1/LF-resistant cell lines are deficient in their ability to activate PA-L1, we used a FRET disruption-based assay (13). Cells were treated with PA-L1 and LF-β-Lac, a β-lactamase enzyme genetically fused to the PA binding domain of LF, and subsequently loaded with the fluorescent β-lactamase substrate CCF-2/AM (13). Melanomas that had activated PA-L1 and internalized LF-β-Lac fluoresced blue from LF-β-Lac mediated substrate cleavage, whereas cells that did not activate PA-L1 fluoresced green (13). PA-L1/LF-β-Lac flow cytometry analysis indicated that the 12 PA-L1/LF-sensitive melanomas all had elevated LF-β-Lac activity (Fig. 1A). Cell lines that were extremely sensitive to PA-L1/LF (IC₅₀ < 20 pmol/L) all showed between 70% and 100% mean blue fluorescence, whereas cells that had an IC₅₀ between 55 and 177 pmol/L showed an intermediate percent mean blue fluorescence. The 6 PA/LF-sensitive, PA-L1/LF-resistant cell lines all exhibited negligible LF-β-Lac activity (Fig. 1B). Moreover, the 7 cell lines that were resistant to both PA/LF and PA-L1/LF, including the low receptor-expressing SK-MEL-2, exhibited variable (low to high) levels of LF-β-Lac activity that were often comparable with the PA-L1/LF-sensitive cell lines (Fig. 1C).

PA-L1/LF-Sensitive Melanomas Exhibit Elevated Cell Surface Gelatinase Activity

To test whether the melanomas that failed to activate PA-L1 expressed low levels of gelatinases, we used gelatin zymography to measure MMP-2 and MMP-9 activity in both melanoma cell conditioned medium and lysates. Conditioned medium zymography analysis determined that neither MMP-2 nor MMP-9 activity correlated with

PA-L1/LF sensitivity (Pearson $r = 0.19$, $P = 0.44$ for MMP-2 and Pearson $r = -0.24$, $P = 0.32$ for MMP-9, respectively; data not shown). Likewise, average conditioned medium gelatinase activity, which was obtained by averaging MMP-2 and MMP-9 percent control values, failed to significantly correlate with melanoma PA-L1/LF sensitivity (Pearson $r = 0.021$, $P = 0.93$). To further support this observation, the addition of 2 ng/well recombinant MMP-2 or MMP-9 to the culture medium did not enhance PA-L1/LF toxicity in the PA/LF-sensitive, PA-L1/LF-resistant cell lines. Furthermore, the addition of both gelatinases to yield an additional 4 ng/well gelatinases in the culture medium did not produce any significant improvement in PA-L1/LF cytotoxicity in these cell lines (data not shown).

Gelatin zymography of cell lysate MMP-2 produced a significant correlation with PA-L1/LF sensitivity (Pearson $r = -0.66$, $P = 0.003$; Fig. 2A), whereas MMP-9 activity did not (Pearson $r = -0.16$, $P = 0.51$; Fig. 2B). Like MMP-2, PA-L1/LF sensitivity showed a significant correlation with average cell lysate gelatinase activity (Pearson $r = -0.61$, $P = 0.006$; Fig. 2C). Representative melanoma cell lines are shown from each group of cell lines in Supplementary Fig. S2.⁷ We also analyzed levels of MT1-MMP (MMP-14) via Western blot because it has been shown previously that MT1-MMP is capable of activating PA-L1 and thus plays a role in PA-L1/LF intoxication (14). However, we found that melanoma cell line MT1-MMP expression did not correlate with PA-L1/LF sensitivity (Pearson $r = -0.019$) (data not shown). MMP-1 has also been shown to be significant in melanoma progression, although expression levels of these MMPs failed to correlate with PA-L1/LF sensitivity (Pearson $r = 0.1528$, $P = 0.5451$; data not shown; ref. 3).

B-RAF Mutational Status in PA/LF-Resistant Melanomas

To explain the cause of the 6 PA/LF-resistant melanoma cell lines, we first determined the B-RAF status of the PA/LF-resistant cell lines by PCR sequencing of exons 11 and 15 of the B-RAF gene, producing the data tabulated in the right-hand column of Table 1. We found that SK-MEL-173, WM239A, and WM3211 did not carry any mutations in either exon 11 or 15. We also found that WM1361A carried the Q61R NRAS mutation. Therefore, these cell lines did not carry the sensitizing V600E B-RAF mutation and thus were not sensitive to LF-mediated MEK cleavage. Furthermore, A2058 was heterozygous for the V600E B-RAF mutation. WM1158, although resistant to PA/LF, was positive for the V600E B-RAF mutation.

Discussion

In this study, 48% of the human melanoma cell lines tested were sensitive to PA-L1/LF. Although our studies indicated that modification of the furin cleavage site did slightly reduce PA potency, we have successfully showed the enhanced selectivity of PA-L1/LF. We were able to show that all PA-L1/LF-sensitive melanoma cell lines exhibited high PA-L1 activation as determined by a FRET disruption-based assay (13). Subsequently, we showed that these cell

⁷ Supplementary materials for this article are available at Molecular Cancer Therapeutics Online (<http://mct.aacrjournals.org/>).

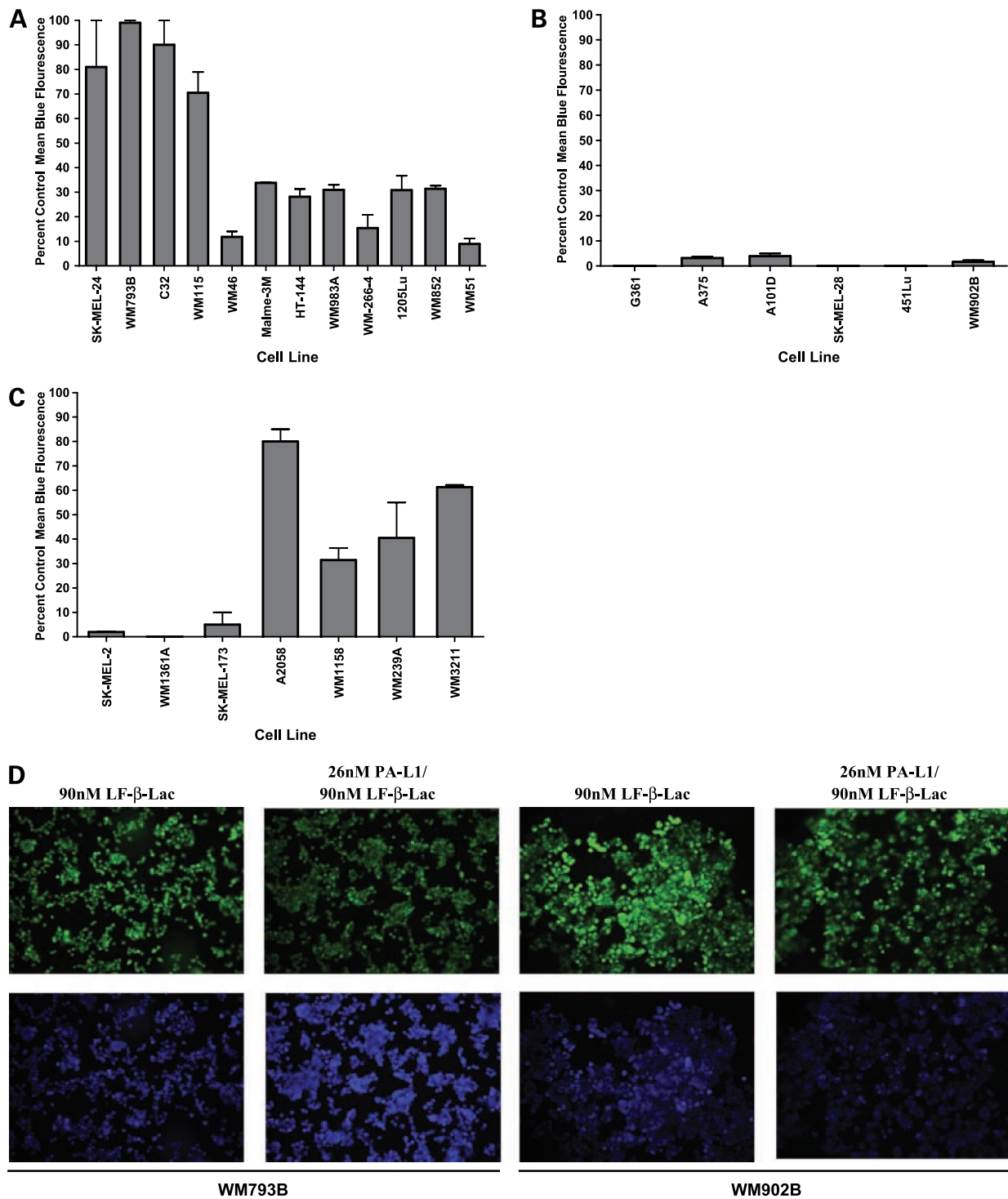


Figure 1. PA-L1 activation by melanoma cells. Melanomas were first treated with either 90 nmol/L LF-β-Lac or 26 nmol/L PA-L1/90 nmol/L LF-β-Lac and then loaded with the β-lactamase enzyme substrate, the membrane-permeable fluorogenic dye CCF-2/AM. Intact CCF-2/AM emits fluorescence at 520 nm (green) due to intramolecular fluorescence resonance transfer between 7-hydroxycoumarin and fluorescein, whereas LF-β-Lac-mediated CCF-2/AM hydrolysis will cause an emission at 447 nm (blue) from the liberated donor coumarin. Melanoma PA-L1 activation and LF-β-Lac internalization will result in blue light emission, whereas cells that did not activate PA-L1 will emit green fluorescence. **A**, PA-L1/LF-β-Lac flow cytometry indicated that PA-L1/LF-β-Lac sensitive melanomas exhibited high LF-β-Lac activity. **B**, all of the PA/LF-sensitive, PA-L1/LF-resistant cell lines showed negligible LF-β-Lac activity. **C**, PA/LF-resistant cell lines showed varying levels of LF-β-Lac activity, with some being comparable with the PA-L1/LF-sensitive cell lines. **D**, PA-L1/LF-sensitive cell line WM793B (PA-L1/LF IC₅₀, 11 pmol/L) and the resistant WM902B (PA-L1/LF IC₅₀, 1,010 pmol/L) were treated with either 90 nmol/L LF-β-Lac alone or 26 nmol/L PA-L1/90 nmol/L LF-β-Lac, loaded with CCF-2/AM, and visualized as described in Materials and Methods. WM793B showed high LF-β-Lac activity, whereas LF-β-Lac activity in WM902B was negligible.

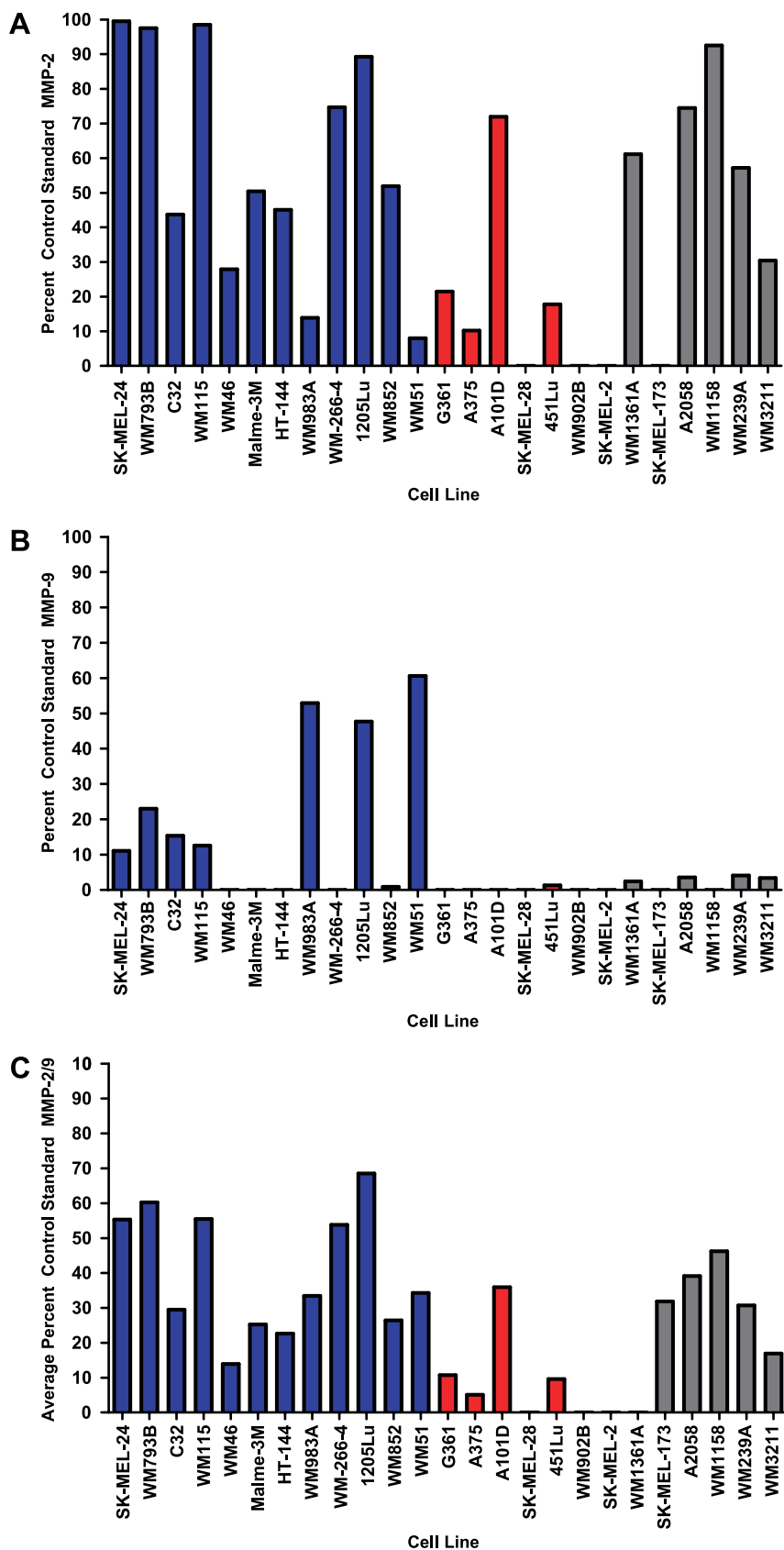


Figure 2. Gelatinase activity in melanoma cell lines. Gelatin zymography was done using recombinant proforms of MMP-2 and MMP-9 (68 and 92 kDa, respectively) and active forms of MMP-2 and MMP-9 (62 and 83 kDa, respectively) as standard controls. Melanoma lysate gelatinase activity was identified as the proform of MMP-2 and MMP-9. Zymography determined that PA-L1-sensitive cells (*blue columns*) overexpressed either (**A**) MMP-2 (**B**) MMP-9 when compared with the PA/LF-sensitive, PA-L1/LF-resistant cell lines (*red columns*). Cell lines that were resistant to PA/LF (*gray columns*) exhibited MMP expression that was comparable with PA-L1/LF-sensitive cell lines. **C**, total gelatinase activity was determined by averaging the percent control standard MMP-2 and MMP-9 activity of each cell line. Representative of two separate experiments.

lines exhibited high cell lysate MMP-2 and/or MMP-9 activity. Furthermore, we showed that 11 of 12 PA-L1/LF-sensitive melanoma cell lines carried the B-RAF V600E mutation. In a study including nonmelanoma human tumors, cells carrying this specific mutation were similarly highly susceptible to LF-mediated MAPK inhibition (11). These results show that the B-RAF V600E is closely associated with sensitivity to LF-mediated cell death. Furthermore, small molecular weight inhibitors of MEK1 show similar B-RAF V600E-dependent melanoma cell cytotoxicity (17). Pathway dependency of tumors has been similarly described with malignancies bearing the Bcr-Abl oncogene and epidermal growth factor receptor mutations (18, 19). Thus, the dual specific recombinant toxin PA-L1/LF requires both the overexpression of MMP-2/9 and the MAPK dependency for antimelanoma efficacy *in vitro*.

Of the 13 PA-L1/LF-resistant melanomas, 6 were dependent on the MAPK pathway for survival as indicated by sensitivity to PA/LF as well as the presence of the V600E B-RAF mutation. These findings suggested that these cells were sensitive to LF-mediated MAPK inhibition but failed to activate PA-L1 and thus did not internalize LF. This PA-L1 activation deficiency was confirmed by the PA-L1 activation assay, which showed that these cells fail to cleave PA-L1. In addition, these melanomas expressed low and sometimes undetectable quantities of cell surface associated MMP-2/9 as determined by lysate zymography.

Taken together, these findings strongly suggest that PA-L1/LF sensitivity is mediated by PA-L1 activation in V600E B-RAF melanomas. Our results indicate that membrane-associated MMP-2/9, but not free gelatinases, MT1-MMP, or membrane-associated MMP-1 and MMP-7 appear to be the primary enzymes involved in PA-L1 cleavage. Proteolytically active MMPs can localize to the cell surface via high affinity binding sites to better direct extracellular matrix degradation (20). MMP-2, aside from being activated on the cell surface via TIMP-2/MT1-MMP complexes, can bind to $\alpha_v\beta_3$ integrins (20, 21). Likewise, CD44 has been shown to serve as a cell surface docking molecule for the localization of MMP-9 (22).

Although lysate MMP-9 activity alone failed to correlate with sensitivity, expression was mostly seen in PA-L1/LF-sensitive and PA/LF-resistant cells. In addition, a select few of the PA-L1/LF-sensitive cells that expressed low levels of MMP-2 overexpressed MMP-9, such as the case with WM983A and WM51. Because initial *in vitro* PA-L1 cleavage studies showed that MMP-9-mediated PA-L1 cleavage efficiency was almost indistinguishable from MMP-2, we could not exclude the significance of this gelatinase in PA-L1 activation (14). Therefore, we reasoned that the activity of MMP-2 and MMP-9 averaged, which did significantly correlate with PA-L1/LF sensitivity, would serve as a more dependable figure for the comparison of gelatinase activity between cell lines. Therefore, V600E melanoma cell lines that have elevated levels of cell surface-associated MMP-2/9 will activate adequate PA-L1 and consequently internalize sufficient quantities of LF for complete MAPK inhibition.

We also found that the remaining 7 melanoma cell lines were resistant to both PA-L1/LF and PA/LF. With the exception of SK-MEL-2, these cells were extremely sensitive to PA/FP59, which indicated adequate LeTx receptor expression for FP59 intoxication. In addition, these cell lines exhibited PA-L1 activation and cell surface associated MMP-2/9 activity that was comparable with that of PA-L1/LF-sensitive melanomas. Taken together, these results indicated that the resistance exhibited by these 6 cell lines was independent of PA-L1 activation and LF internalization. In an attempt to determine the cause of resistance in this group of cell lines, we determined whether the sensitizing V600E B-RAF mutation was present. Our results indicated that 3 of the PA/LF-resistant melanomas did not carry any mutations in exon 11 or 15 in the B-RAF gene and 1 melanoma carried a mutation in the upstream NRAS. In addition, 1 cell line harbored a heterozygous mutation in the B-RAF gene. Therefore, these cells do not express, or only partially express, the constitutively active B-RAF protein. As a result, these cell lines are not sensitive to MAPK inhibition.

However, we found that WM1158 was positive for the V600E B-RAF mutation. We determined whether the phosphatidylinositol 3-kinase/PTEN/Akt/GSK3 β pathway had a role in the observed PA/LF resistance. It has recently been shown that the activation of Akt causes the inhibition of GSK3 β -mediated cyclin D1 degradation and consequential G₀-G₁ cell cycle arrest (23). This activation is critical for recovery from LeTx-mediated cell cycle arrest and resistance to subsequent toxin challenge in human macrophages (23). Furthermore, Akt overactivation can result from the loss of the lipid phosphatase PTEN in melanomas (24). Therefore, we reasoned that the activation of Akt, possibly through the deletion of PTEN, could potentially provide WM1158 cells a LF-mediated MEK cleavage bypass mechanism (24, 25). We found that although WM1158 PTEN expression was not detectable via Western blot, the pretreatment of WM1158 cells with either phosphatidylinositol 3-kinase or Akt inhibitors failed to enhance PA/LF cytotoxicity. Furthermore, the inhibition of GSK3 β did not increase the resistance in PA/LF-sensitive 451Lu cells. Thus, resistance mechanisms to PA/LF in B-RAF V600E/MMP-2/9-overexpressing melanoma cells are currently not defined. As noted in previous work from our laboratory, the presence of the V600E B-RAF mutation does not always translate to sensitivity to LF-mediated MEK cleavage (10). However, only 1 of 19 V600E B-RAF melanomas was resistant to LF-mediated MAPK inhibition, which makes this type of resistance rare.

In conclusion, we have showed that both adequate cell surface-associated MMP-2/9 and the MAPK-activating V600E B-RAF mutation are needed in order for PA-L1/LF to be active. This dual specificity has already showed a 3-fold higher LD₁₀ in addition to a 20-fold greater circulating half-life when compared with LeTx (11). As a result, *in vivo* antitumor efficacy was dramatically improved by an elevated area under the curve from a higher dose and longer half-life (11). Moreover, we have shown that cell

surface-associated MMP-2/9 activity significantly correlates with PA-L1/LF sensitivity and therefore is the primary mediator in sensitivity among V600E B-RAF melanomas *in vitro*. The contribution of this mechanism to the overall antitumor mechanism of PA-L1/LF *in vivo* remains unclear, because PA-L1/LF has been shown to induce endothelial dysfunction during angiogenesis (11, 26). However, this correlation of *in vitro* cytotoxicity to MMP-2/9 expression permits the application of simple biomarker assays on tumor samples for prediction of patient response to PA-L1/LF. Therefore, we propose tumor tissue PCR and sequencing for B-RAF V600E status and immunohistochemistry for expression of MMP-2 and MMP-9 (27–29). Taken together, these findings will ultimately aid in the selection of metastatic melanoma patients for systemic MMP-activated LeTx therapy.

Disclosure of Potential Conflicts of Interest

S.H. Leppla, S. Liu: named inventors on patents and patent applications held by the U.S. government on related technologies. The other authors reported no potential conflicts of interest.

Acknowledgments

We thank Drs. Jen-Sing Liu and Shu-Ru Kuo for helpful discussions and Alan Houghton for SK-MEL-173; Dr. Honying Zheng, Dr. Juhee Song, and Courtney Ireland for technical assistance; and Drs. Yunpeng Su and Cindy Meininger for critical reading of the article.

References

- Queirolo P, Acquati M. Targeted therapies in melanoma. *Cancer Treat Rev* 2006;32:524–31.
- Davies H, Bignell GR, Cox C, et al. Mutations of the BRAF gene in human cancer. *Nature* 2002;417:949–54.
- Hofmann UB, Houben R, Bröcker EB, Becker JC. Role of matrix metalloproteinases in melanoma cell invasion. *Biochimie* 2005;87:307–14.
- Denkert C, Siegert A, Leclere A, Turzynski A, Hauptmann S. An inhibitor of stress-activated MAP-kinases reduces invasion and MMP-2 expression of malignant melanoma cells. *Clin Exp Metastasis* 2002;19:79–85.
- Duesbery NS, Resau J, Webb CP, et al. Suppression of ras-mediated transformation and inhibition of tumor growth and angiogenesis by anthrax lethal factor, a proteolytic inhibitor of multiple MEK pathways. *Proc Natl Acad Sci U S A* 2001;98:4089–94.
- Young JA, Collier RJ. Anthrax toxin: receptor binding, internalization, pore formation, and translocation. *Annu Rev Biochem* 2007;76:243–65.
- Puhar A, Montecucco C. Where and how do anthrax toxins exit endosomes to intoxicate host cells? *Trends Microbiol* 2007;15:477–82.
- Chopra AP, Boone SA, Liang X, Duesbery NS. Anthrax lethal factor proteolysis and inactivation of MAPK kinase. *J Biol Chem* 2003;278:9402–6.
- Koo HM, VanBrocklin M, McWilliams MJ, Leppla SH, Duesbery NS, Vande Woude GF. Apoptosis and melanogenesis in human melanoma cells induced by anthrax lethal factor inactivation of mitogen-activated protein kinase kinase. *Proc Natl Acad Sci U S A* 2002;99:3052–7.
- Abi-Habib RJ, Urieto JO, Liu S, Leppla SH, Duesbery NS, Frankel AE. BRAF status and mitogen-activated protein/extracellular signal-regulated kinase kinase 1/2 activity indicate sensitivity of melanoma cells to anthrax lethal toxin. *Mol Cancer Ther* 2005;4:1303–10.
- Liu S, Wang H, Currie BM, et al. Matrix metalloproteinase-activated anthrax lethal toxin demonstrates high potency in targeting tumor vasculature. *J Biol Chem* 2008;283:529–40.
- Chen KH, Liu S, Bankston LA, Liddington RC, Leppla SH. Selection of anthrax toxin protective antigen variants that discriminate between the cellular receptors TEM8 and CMG2 and achieve targeting of tumor cells. *J Biol Chem* 2007;282:9834–45.
- Hobson JP, Liu S, Rono B, Leppla SH, Bugge TH. Imaging specific cell-surface proteolytic activity in single living cells. *Nat Methods* 2006;3:259–61.
- Liu S, Netzel-Arnett S, Birkedal-Hansen H, Leppla SH. Tumor cell-selective cytotoxicity of matrix metalloproteinase-activated anthrax toxin. *Cancer Res* 2000;60:6061–7.
- Arora N, Klimpel K, Singh Y, Leppla S. Fusions of anthrax toxin lethal factor to the ADP-ribosylation domain of *Pseudomonas* exotoxin A are potent cytotoxins which are translocated to the cytosol of mammalian cells. *J Biol Chem* 1992;267:15542–8.
- Wong L, Suh DY, Frankel AE. Toxin conjugate therapy of cancer. *J Seminoncol* 2005;8:591–5.
- Sharma A, Tran MA, Liang S, et al. Targeting mitogen-activated protein kinase/extracellular signal-regulated kinase kinase in the mutant (V600E) B-Raf signaling cascade effectively inhibits melanoma lung metastases. *Cancer Res* 2006;66:8200–9.
- Sequist LV, Lynch TJ. EGFR tyrosine kinase inhibitors in lung cancer: an evolving story. *Annu Rev Med* 2008;59:429–42.
- White D, Saunders V, Grigg A, et al. Measurement of *in vivo* BCR-ABL kinase inhibition to monitor imatinib-induced target blockade and predict response in chronic myeloid leukemia. *J Clin Oncol* 2007;25:4445–51.
- Hofmann U, Westphal J, Van Muijen G, Ruiter D. Matrix metalloproteinases in human melanoma. *J Invest Dermatol* 2000;115:337–44.
- Hornebeck W, Emonard H, Monboisse J, Bellon G. Matrix-directed regulation of pericellular proteolysis and tumor progression. *Semin Cancer Biol* 2002;12:231–41.
- Yu Q, Stamenkovic I. Localization of matrix metalloproteinase 9 to the cell surface provides a mechanism for CD44-mediated tumor invasion. *Genes Dev* 1999;13:35–48.
- Ha SD, Ng D, Pelech S, Kim SO. Critical role of PI3-K/Akt/GSK-3 β signaling pathway in recovery from anthrax lethal toxin-induced cell cycle arrest and MEK cleavage in macrophages. *J Biol Chem* 2007;282:36230–9.
- Haluska FG, Tsao H, Wu H, Haluska FS, Lazar A, Goel V. Genetic alterations in signaling pathways in melanoma. *Clin Cancer Res* 2006;12:2301–7s.
- Tsao H, Goel V, Wu H, Yang G, Haluska FG. Genetic interaction between NRAS and BRAF mutations and PTEN/MMAC1 inactivation in melanoma. *J Invest Dermatol* 2004;122:337–41.
- Alfano RW, Leppla SH, Bugge TH, Duesbery NS, Frankel AE. Potent inhibition of tumor angiogenesis by the matrix metalloproteinase-activated anthrax lethal toxin: implications for broad anti-tumor efficacy. *Cell Cycle* 2008;7. Epub ahead of print.
- Gorden A, Osman I, Gai W, et al. Analysis of BRAF and N-RAS mutations in metastatic melanoma tissues. *Cancer Res* 2003;63:3955–7.
- Simonetti O, Lucarini G, Brancorsini D, et al. Immunohistochemical expression of vascular endothelial growth factor, matrix metalloproteinase 2, and matrix metalloproteinase 9 in cutaneous melanocytic lesions. *Cancer* 2002;95:1963–70.
- Spittle C, Ward MR, Nathanson KL, et al. Application of a BRAF pyrosequencing assay for mutation detection and copy number analysis in malignant melanoma. *J Mol Diagn* 2007;9:464–71.
- Smalley K, Contractor R, Haass N, et al. Ki67 expression levels are a better marker of reduced melanoma growth following MEK inhibitor treatment than phospho-ERK levels. *Br J Cancer* 2007;96:445–9.